

PACS 42.65.Ky, 85.60.-q, 07.05.Tp

Electro-optic effect in GaN/Al_{0.15}Ga_{0.85}N single quantum wells for optical switch

A. Elkadadra, D. Abouelaoualim^{*}, A. Oueriagli, A. Outzourhit

LPSCM, Department of Physics, Faculty of Sciences Semlalia

Cadi Ayaad University P.O. Box 2390, 40000 Marrakech, Morocco

**Corresponding author: abouelaoualim_d@hotmail.com*

Abstract. The second-harmonic generation (SHG) susceptibility of wurtzite type gallium nitride with single quantum wells has been theoretically investigated in the framework of the compact-density-matrix approach. The confined wave functions and energies of electrons in GaN/Al_xGa_{1-x}N have been calculated in the effective-mass approximation, solving the Schrödinger equation by Numerov's method using the second and fourth order approximations for the derivatives. The numerical results for typical GaN/Al_{0.15}Ga_{0.85}N quantum wells show that a strong SHG effect can be realized in electric field by choosing some optimized structural parameters.

Keywords: second-harmonic generation, wurtzite quantum well, effects of electric field, density matrix approach, Numerov's method.

Manuscript received 19.05.10; accepted for publication 08.07.10; published online 30.09.10.

1. Introduction

In the recent few years, nonlinear optical properties in the low-dimensional semiconductor quantum systems, such as quantum wells [1-5], quantum wires [6, 7] and quantum dots [8, 9], have attracted much attention both in practical applications and in theoretical research. By one reason, the nonlinear effects in these low-dimensional quantum systems can be enhanced more dramatically over those in bulk materials due to existence of a strong quantum-confinement effect. By another one, these nonlinear properties have the potential for device application in far-infrared laser amplifiers, photodetectors, electro-optical modulators and all-optical switches. In addition, the fast development of graving technologies such as molecular beam epitaxy and metal-organic chemical vapor deposition has also accelerated researches in this area.

Recently, there has been a considerable interest in interband transitions (IBTs) in nitride semiconductor quantum well (QW) structures [10-15] the possibility of achieving both linear and nonlinear optical properties. Also, IBTs in nitride semiconductor QWs have been the subject of extensive researches for their extremely large oscillator strengths and relatively narrow line widths, and are used in a variety of optoelectronic devices like QW infrared lasers [16, 17], switches and MQW electrooptical modulators [18]. Above all, nitride-

semiconductor heterostructures have several advantages, namely: (1) the absorption recovery time is considerably lower than 1 ps, (2) a wide range of wavelengths is available with a less-complicated quantum structure, (3) the homogeneous line width is sufficiently broad due to the short dephasing time, (4) two-photon absorption does not interfere with the saturable absorption due to the wide band-gap [19, 20].

In this paper, we show that the electric field breaks the symmetry of the confinement potential profile and leads to large second-order susceptibilities in a wurtzite GaN/Al_xGa_{1-x}N QW.

The organization of this paper is as follows. In Section 2, theory and model are presented. The model of calculation used in this paper is based on using the effective mass Schrödinger with the Numerov numerical technique that we provide. Simulation results of our models and discussions are illustrated in Section 3. In this section, our results have been explained and show that the proposed structure is a better model for applications in microwave and optical switches. Finally, the paper contains a short conclusion.

2. Theory and model

Using the density-matrix formalism, the second-harmonic generation (SHG) susceptibility of the double frequency 2ω in a bulk material or quantum confined

systems by an incident optical beam with the frequency ω . Assuming a monochromatic incident electromagnetic field $E(t) = E \exp(-i\omega t) + E^* \exp(i\omega t)$ is applied to a system, the polarization response is written as [20, 21].

$$\chi_{2\omega}^{(2)} = \frac{q^3}{\varepsilon_0 \hbar^2} \sum_i \sum_k \frac{1}{(2\omega + \omega_{ki}) - i\Gamma_{ki}} \times \sum_l \mu_{ik} \mu_{kl} \mu_{li} \left[\frac{\rho_i - \rho_l}{(\omega + \omega_{li}) - \Gamma_{li}} - \frac{\rho_l - \rho_k}{(\omega + \omega_{kl}) - \Gamma_{kl}} \right] \quad (1)$$

In the two-level structure, only two terms remain in the summation, namely: those for which $k = 1$, $i = 2$ and $l = 1$ or 2 . This yields for the quadratic susceptibility $\chi_{2\omega}^{(2)}$:

$$\chi_{2\omega}^{(2)} = \frac{q^3 (N_1 - N_2)}{\varepsilon_0 \hbar^2} \frac{z_{12}^2 \delta_{12}}{(\omega - \omega_{21} - i\Gamma_2)(2\omega - \omega_{21} - i\Gamma_2)}, \quad (2)$$

where $\delta_{12} = \langle 2 | \hat{z} | 2 \rangle - \langle 1 | \hat{z} | 1 \rangle = z_{22} - z_{11}$ is the average electron displacement resulting from the transition from the level $|1\rangle$ to $|2\rangle$. N_1 and N_2 are the electron density in the respective levels $|1\rangle$ and $|2\rangle$. Γ_1 and Γ_2 are, respectively, the population relaxation rate (inelastic mechanism) and dephasing constant corresponding to elastic scattering. Far from resonance ($\omega_{12} \gg \omega$), it can be written:

$$\chi_{2\omega}^{(2)} = \frac{q (n_1 - n_2) (z_{12}^2 \delta_{12})}{\varepsilon_0 (\hbar \omega_{21} / q)^2}. \quad (3)$$

Eq. (2) requires the energies and wave functions of the QW structure, which can be obtained solving the Schrödinger equation.

The schematic diagram for the electron confined potential profile in QW is shown in Fig. 1. The effective mass Hamiltonian for the electron in this coupled quantum system is given as

$$-\frac{\hbar^2}{2} \frac{d}{dz} \left(\frac{d}{dz} \frac{1}{m(z)} \right) \varphi(z) + V(z) \varphi(z) = E \varphi(z). \quad (4)$$

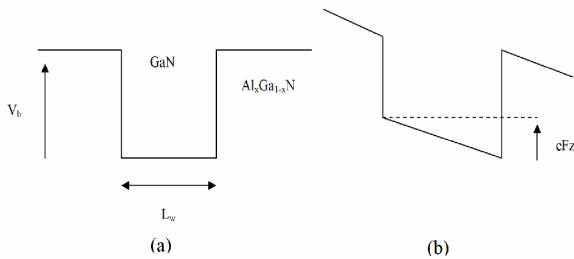


Fig. 1. Schematic diagram for electron confined potential profile for GaN/Al_xGa_{1-x}N strained single quantum well, (a) without any electric field, (b) under the electric field F_z .

When the Schrödinger equation is solved using a simple but highly accurate numerical technique [23], the envelope wave function of Eq. (4) can be written in the following form:

$$\varphi(z) = \begin{cases} \varphi_{b_1}(z) = A e^{\alpha z}, & z < 0, \\ \varphi_w(z), & 0 \leq z \leq w, \\ \varphi_{b_2}(z) = B e^{-\beta z}, & z \geq w. \end{cases} \quad (5)$$

Here

$$\alpha = \sqrt{\frac{2m_b^*(V_1 - E)}{\hbar^2}}, \quad \beta = \sqrt{\frac{2m_b^*(V_2 - E)}{\hbar^2}}, \quad (6)$$

where m_b^* is the effective mass of the particle at the barrier, and the overall potential can be presented as follows (Eq. (7)):

$$V(z) = E_c(z) - eF_z z, \quad (7)$$

where $E_c(z)$ represents the conduction-band profile given by the material compositions, and F_z is the electric field applied to the structure along the axis z . We integrate the Schrödinger equation by a two-step numerical method. First, one is to find the iterative formula. We add the fourth- and sixth-order derivatives to raise precision of the traditional Numerov method [23-26] from the fourth order to the twelfth order, and to expand the interval of periodicity. The second step is to find the mated first-order derivative formula, and the latter is to give the algorithm.

3. Numerical results and discussion

In this section, simulation results are presented and discussed, which characterize the electrical and optical properties of GaN/Al_xGa_{1-x}N single quantum well structure for the aluminium concentration $x = 0.15$, when the quantum well width is $L_w = 80$ Å. The dephasing constant corresponding to elastic scattering is $\Gamma_2 = 0.14$ ps. The optimal doping concentration is $N_d = 10^{24}$ cm⁻³. Material parameters and values of polarization and elastic constants used in the calculation are given in Table 1 [27].

Table 1. Material parameters and values of polarization and elastic constants used in the calculation.

Parameter	Unit	GaN	Al _x Ga _{1-x} N
a	Å	3.189	$3.122x + 3.189(1-x)$
ε_r	F/m	10	$0.58x + 10(1-x)$
Conduction band effective masses m^*/m_0	–	0.19	$0.19(1-x) + 0.33x$
Band gap ($E_g(x)$)	eV	3.475	$6.13x + (1-x) 3.42 - x(1-x)$
Band offset ($\Delta E_c(x)$)	eV	–	$0.7[E_g(x) - E_g(0)]$

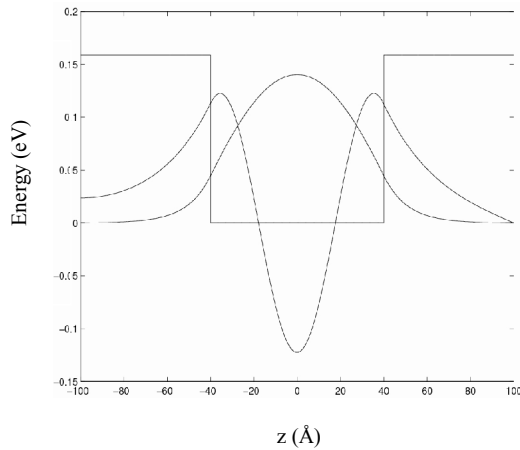


Fig. 2. Schematic diagrams of wave functions for an electron confined in GaN/Al_{0.15}Ga_{0.85}N QW.

Using the Numerov method to numerically solve the Schrödinger equation (Eq. (4)) in one dimension, we find both the eigenvalues and the wave functions. The efficiency of Numerov's method lies in the fact that one obtains a local error of $O(h^6)$ with just one evaluation of V and E per one step. This should be compared to the Runge–Kutt algorithm that needs six function evaluations per step to achieve a local error of $O(h^6)$. In Fig. 2, not only the confined potential profile of the conduction band electron, but also the electron wave functions of the ground-state φ_1 for the first excited state φ_2 for the second excited one in z -direction are plotted without the electric field F . Here we see the symmetry of wave functions relatively to the center of this QW structure.

The Fig. 3 illustrates the electric field effect on wave functions for electron confined in the quantum well. Three special values of F were used.

We can see from Fig. 3 that the strong F in GaN/Al_{0.15}Ga_{0.85}N QW can induce a remarkable change of the electron wave function spatial distribution. So, the applications of an electric field perpendicular to the plane of the QW influence its electron properties. It increases the quantum confined effect. It should be noted that the situation is quite different when considering the quantum confined electron and hole wave functions in QW. At flat band condition (zero-field), a QW is simply treated as a quantum mechanical “particle-in-a-box”, wherein the electron have symmetric trigonometrical sinusoidal wave functions from which the energy of intraband transitions can be easily obtained. With electric field, band bending occurs, forming a tilted quantum well which results in lowering the energy of band transitions, i.e., the electron subband energy level drops. This band bending is a result of self-consistency of this problem. Thus, the symmetry is broken.

In the second part, the effect of electric field on the second-order susceptibility has been presented. This susceptibility has been calculated for two state transitions. In Fig. 4, we plot the second-order susceptibility $\chi^{(2)}$ as a function of the photon energy $\hbar\omega$ for different values of electric field.

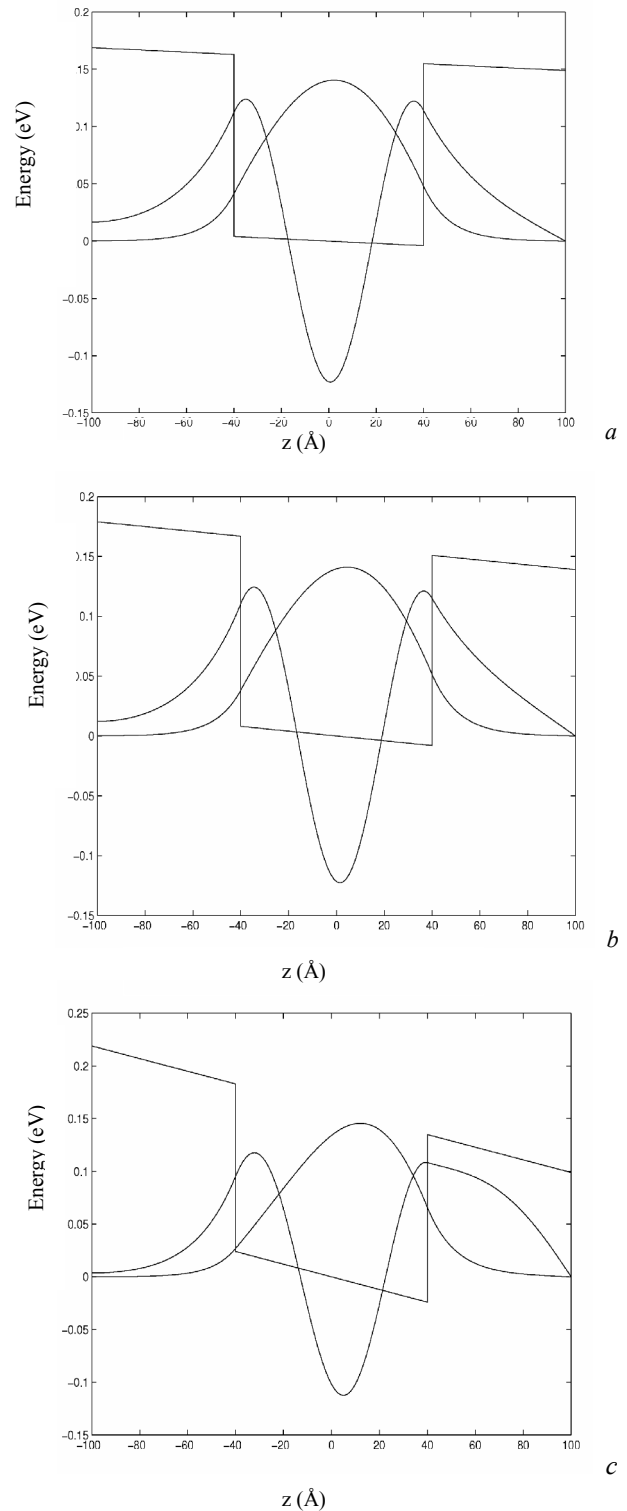


Fig. 3. Schematic diagrams of wave functions for an electron confined in GaN/Al_{0.15}Ga_{0.85}N QW for different values of the electric field: $F = 10$ (a), 20 (b) and 60 kV/cm (c).

From Fig. 4, we observe that $\chi^{(2)}$ increases with increasing the electric field. The peak of the susceptibility increases (the whole range of variations are: from 10^{-10} to 10^{-4}), which can be attributed to the

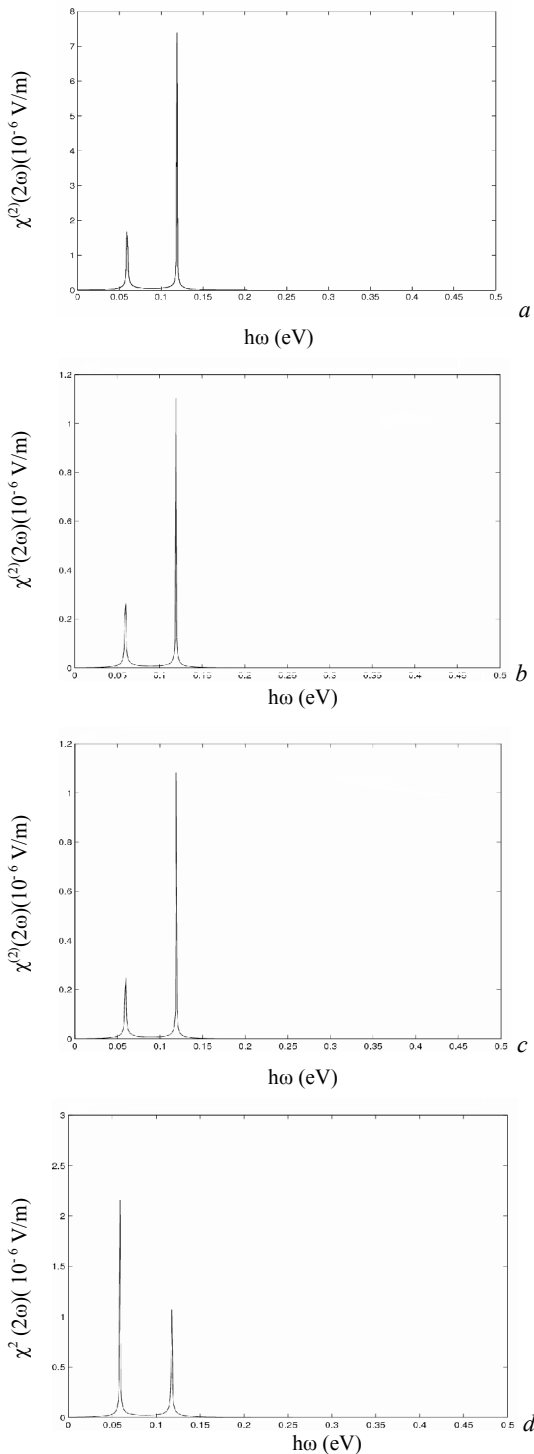


Fig. 4. $\chi^{(2)}(2\omega)$ as a function of the pumping photo-energy $h\omega$. F values are equal to: 0 (a), 10 (b), 20 (c) and 60 kV/cm (d).

strong confinement of the electron due to electric field. This conversion of peak proportions can cause band bending with increasing the electric field. It is therefore possible to manage the resonant frequency and the amplitude of sensitivity of the second order with a suitable choice of the quantum well width ($L_w = 80 \text{ \AA}$), which plays an important role in the confinement of electrons in the quantum well structure.

4. Conclusion

In conclusion, taking the strong effect of built-in electric field into account, the second-harmonic generation (SHG) susceptibility in a GaN/Al_{0.15}Ga_{0.85}N QW system has been theoretically analyzed, and the Numerov numerical technique to solve Schrödinger equation has been used. A large value of $\chi^{(2)}$ (several orders than that of bulk GaN) has been obtained, which can be used for the wavelength conversion in optical switches.

References

1. Xiaoqin Li, Tianhao Zhang, Shaul Mukamel, Richard P. Mirin, Steven T. Cundiff // *Solid State Communs.* **149**, p. 361-366 (2009).
2. Jiunn-Chyi Lee, Ya-Fen Wu // *Thin Solid Films*, In Press, Accepted Manuscript, Available online 10 May (2010).
3. D.R. Luhman, W. Pan, D.C. Tsui, L.N. Pfeiffer, K.W. Baldwin, K.W. West // *Physica E*, **40**, p. 1059-1061 (2008).
4. Sankha S. Mukherjee, Syed S. Islam // *Superlattices and Microstructures*, **41**, p. 56-61 (2007).
5. D.R. Luhman, W. Pan, D.C. Tsui, L.N. Pfeiffer, K.W. Baldwin, K.W. West // *Physica E*, **40**, p. 1059-1061 (2008).
6. R. Khordad, A. Gharaati, M. Haghparast // *Curr. Appl. Phys.* **10**, p. 199-202 (2010).
7. D. Abouelaoualim // *Acta Phys. Pol. A*, **112**, p. 49-54 (2007).
8. A.A. Lagatsky, C.G. Leburn, C.T.A. Brown, W. Sibbett, S.A. Zolotovskaya, E.U. Rafailov // *Progr. Quant. Elect.*, **34**, p. 1-45 (2010).
9. Dirk Englund, Ilya Fushman, Andrei Faraon, Jelena Vučković // *Photonics and Nanostructures*, **7**(1), p. 56-62 (2009).
10. S.C.P. Rodrigues, O.F.P. dos Santos, L.M.R. Scolfaro, G.M. Sipahi, E.F. da Silva Jr // *Appl. Surf. Sci.*, **254**, p. 7790-7793 (2008).
11. A. Freundlich, A. Fotkatzikis, L. Bhusal, L. Williams, A. Alemu, W. Zhu, J.A.H. Coaquira, A. Feltrin, G. Radhakrishnan // *J. Cryst. Growth*, **301-302**, p. 993-996 (2007).
12. A. Alemu, A. Freundlich // *Microelectronics J.*, **40**, p. 421-423 (2009).
13. A. Molina, A. García-Cristóbal, A. Cantarero // *J. Microelectronics*, **40**, p. 418-420 (2009).
14. S.M. Wang, H. Zhao, G. Adolfsson, Y.Q. Wei, Q.X. Zhao, J.S. Gustavsson, M. Sadeghi, A. Larsson // *Microelectronics J.*, **40**, p. 386-391 (2009).
15. Mikhail V. Kisin, Hussein S. El-Ghoroury // *Solid-State Electron.*, In Press, Corrected Proof, Available online 1 May 2010.
16. Guijun Hu, Jing Li, Yingxue Shi, Jiawei Shi // *Opt. & Laser Technol.*, **39**, p. 165-168 (2007).
17. N. Eseau // *Phys. Lett. A*, **374**, p. 1278-1285 (2010).

18. Hsin-Ying Lee, Tsung-Hsin Lee, Wen-Tron Shay, Ching-Ting Lee // *Sensors and Actuators A: Phys.*, **148**, p. 355-358 (2008).
19. P.K. Chakraborty, S. Ghoshal, K.P. Ghatak // *Physica B*, **382**, p.26-37 (2006).
20. J.H. Yu, J.H. Kim, D.S. Park et al. // *J. Cryst. Growth*, **312**, p. 1683-1686 (2010).
21. Li Zhang // *Superlattices and Microstructures*, **37**, p. 261-272 (2005).
22. Y. Wen, G.G. Xiong, Q.Q. Wang, D.J. Chen // *Physica B*, 370, p. 195 (2005).
23. Salvador Jiménez, Ignacio M. Llorente, Ana M. Mancho, Víctor M. Pérez-García, Luis Vázquez // *Appl. Math. Computations*, **134**, p. 271-291 (2003).
24. R. P. Agarwal, Yuan-Ming Wang // *Computers Math. Appl.* **42**, p. 561-592 (2001).
25. G. Vanden Berghe, M. Van Daele // *J. Comput. Appl. Math.* **200**, p. 140-153 (2007).
26. Yonglei Fang, Yongzhong Song, Xinyuan Wu // *Comput. Phys. Commun.* **179**, p. 801-811 (2008).
27. F. Bernardini, V. Fiorentini // *Phys. Rev. B*, **64**, p. 5207 (2001).